

# LCST in poly(*N*-isopropylacrylamide) copolymers: high resolution proton NMR investigations

M.V. Deshmukh<sup>a</sup>, A.A. Vaidya<sup>b</sup>, M.G. Kulkarni<sup>b</sup>, P.R. Rajamohanam<sup>a</sup>, S. Ganapathy<sup>a,\*</sup>

<sup>a</sup>Physical Chemistry Division, National Chemical Laboratory, Pune 411 008, India

<sup>b</sup>Chemical Engineering Division, National Chemical Laboratory, Pune 411 008, India

Received 12 October 1999; received in revised form 4 February 2000; accepted 14 February 2000

## Abstract

A series of copolymers of *N*-isopropylacrylamide (NIPA) and acryloyl amino acids were synthesized and conjugated with *p*-aminobenzamidine (PABA). The values of lower critical solution temperatures (LCSTs) of these polymers estimated by <sup>1</sup>H NMR were in agreement with those estimated by the turbidometric methods. The apparent shifts in the peak positions for the polymer with increasing temperature reported in the past are shown to be artifacts resulting from the deuterium lock experiment. The <sup>1</sup>H–<sup>1</sup>H NOESY experiments were carried out to distinguish the interactions between the protons in: (a) 6-amino caproic acid (6ACA) and NIPA and (b) PABA and NIPA. These explain the variation in the LCST of the polymers based on the contributions of the two monomers to the magnitude of the polymer–polymer interactions. The findings are further supported by proton spin–lattice relaxation time measurements. © 2000 Elsevier Science Ltd. All rights reserved.

**Keywords:** *N*-isopropylacrylamide; Lower critical solution temperature; <sup>1</sup>H NMR

## 1. Introduction

Poly(*N*-isopropylacrylamide), poly(NIPA), belongs to a class of polymers, which undergo a transition from the hydrophilic to hydrophobic state with increasing temperature and hence exhibit inverse temperature dependence of solubility [1,2]. The realization that materials of this kind could find wide ranging applications in separations, drug delivery, enzyme conjugation and photo switching, provided further impetus to investigate their structural features which influence the lower critical solution temperature (LCST) behaviour of these polymers, so as to enable us to design more efficient polymers for these applications [3,4].

We have been investigating the role of polymer structure in enhancing the recovery of enzymes by affinity precipitation. We synthesized the copolymers of *N*-isopropylacrylamide and *N*-acryloyl amino acids. *p*-Aminobenzamidine was chemically linked to the terminal carboxyl group of the amino acid to obtain thermo precipitating affinity polymers for the selective recovery of trypsin. The choice of the amino acid governed the LCST of the polymer as well as the

recovery and activity of trypsin recovered. While the incorporation of the amino acid led to the lowering of LCST, the conjugation of amino acid with *p*-aminobenzamidine resulted in an enhancement of the LCST of the polymer [5].

For practical applications, it is crucial that the thermo-precipitating polymers be tailored in such a way that the LCST lies in the vicinity of the room temperature. Previous investigations have indicated that poly(*N*-isopropylacrylamide) and its copolymers undergo concomitant intra-chain coil to globule transition and inter-chain aggregation [6]. An understanding of the nature of interactions within the polymer structure would help understand the variation of LCST with polymer structure on a more rational basis [7].

In this paper we report the results of the high resolution proton NMR investigations of a series of copolymers of *N*-isopropylacrylamide and acryloyl amino acids as well as their *p*-amino benzamidine conjugates. The temperature dependence of proton NMR resonance of poly(*N*-isopropylacrylamide-*co*-acryloyl 6 amino caproic acid, 90:10) (poly(NIPA-*co*-Ac-6ACA, 90:10)) indicates an LCST of 28°C which is in close agreement with the value obtained by the turbidometric method. The <sup>1</sup>H–<sup>1</sup>H 2D NOESY experiments were carried out to distinguish between the various interactions in poly(NIPA), poly(NIPA-*co*-Ac-6ACA) and poly(NIPA-*co*-Ac-PABA). In poly(NIPA-*co*-Ac-6ACA, 90:10), the interactions between the α-protons

\* Corresponding author. Tel.: +91-20-5893300; fax: +91-20-5893355.

E-mail address: ganpat@ems.ncl.res.in (S. Ganapathy).

in 6ACA and the main chain and side chain protons in NIPA dominate, leading to an increase in the hydrophobicity. The analysis of the NOESY data indicates that the intra-chain interactions in poly(NIPA-*co*-Ac-6ACA, 80:20) are stronger than those in poly(NIPA-*co*-Ac-PABA, 70:30). This explains why the LCST of poly(NIPA-*co*-Ac-6ACA, 80:20) is lower than that of poly(NIPA-*co*-Ac-PABA, 70:30). The proton spin–lattice relaxation time ( $T_1$ ) measurements did not show any definite trend. Incorporation of both Ac-6ACA and Ac-PABA decreases  $T_1$  of all the protons. The hydrophobic 6ACA moiety affects the proton  $T_1$ s more than the hydrophilic PABA moiety.

## 2. Materials

Acrylic acid, 6-amino caproic acid (6ACA), *p*-amino benzamide dihydrochloride (PABA.2HCl), 1-cyclohexyl-3-(2-morpholinoethyl) carbodiimide metho-*p*-toluenesulfonate (CMC), *N*-isopropylacrylamide (NIPA), and 11-amino undecanoic acid (11AUA) were obtained from Aldrich. 4-Amino butyric acid (4ABA),  $\beta$ -Alanine ( $\beta$ -Ala), glycine (Gly), thionyl chloride, ammonium persulfate, tetramethylethylenediamine (TEMED), etc. were obtained from local suppliers. The solvents used in this work were of analytical grade.

## 3. Methods

### 3.1. Synthesis of *N*-acryloyl *p*-aminobenzamide (Ac-PABA)

Acryloyl chloride was synthesized by the reaction of thionyl chloride and acrylic acid. *N*-acryloyl *p*-aminobenzamide (Ac-PABA) was synthesized by the reaction of acryloyl chloride and PABA.2HCl [8,9].

### 3.2. Synthesis of *N*-acryloyl 6 amino caproic acid (Ac-6ACA)

Ac-6ACA was synthesized as described below. In a 250 ml beaker equipped with a dropping funnel and pH meter, 13.16 g 6ACA (0.1 M), 4 g NaOH (0.1 M) and 80 ml water were placed to obtain a clear solution (pH 13). This was stirred at 5–10°C on a magnetic stirrer. Nine-milliliter acryloyl chloride (0.11 M) in 10 ml dichloromethane was added dropwise to the above solution over a period of 45–60 min. During this period the pH of the reaction mixture was maintained in the range 7.4–7.8 by adding 10 M NaOH solution. After the addition was over and the pH of the reaction mixture was steady, unreacted acid chloride was extracted in 100 ml ethyl acetate. The clear aqueous solution was acidified to pH 5.0 by adding concentrated HCl and the product was extracted in ethyl acetate (3 × 100 ml). The organic layer was dried on anhydrous sodium sulfate and concentrated under vacuum. The viscous liquid

obtained was poured in 500 ml petroleum ether. This was kept in a refrigerator for 4–5 days with occasional scratching in order to obtain a solid product. Yield—56%. M.P. 77–78°C.

All other *N*-acryloyl amino acids were similarly synthesized. Only in the case of *N*-acryloyl- $\beta$ -alanine and *N*-acryloyl glycine the products were obtained by precipitation of aqueous solutions in acetone and purified by reprecipitation from methanol into acetone.

*N*-acryloyl-4-amino butyric acid (Ac-4ABA); yield—55%, M.P. 90–91°C.

*N*-acryloyl- $\beta$ -alanine (Ac- $\beta$ -Ala); yield—40%, M.P. 128–130°C.

*N*-acryloyl glycine (Ac-Gly); yield—35%, M.P. 127–128°C.

*N*-acryloyl-11-undecanoic acid (Ac-11AUA); yield—65%, M.P. 237–238°C.

### 3.3. Synthesis of *N*IPA–acryloyl amino acid copolymers

0.01 M of the acryloyl amino acid and 0.09 M of NIPA were dissolved in 50 ml water. To this, 10% w/w ammonium persulfate was added and the solution was purged with nitrogen for 15 min. Polymerization was initiated by adding 500  $\mu$ l of TEMED and was allowed to proceed at 37°C for 18 h. The polymer so synthesized was precipitated by increasing the temperature above its LCST. The polymer was washed twice with cold double distilled water and dried under vacuum at room temperature. The same procedure was used for the synthesis of: (1) poly(*N*-isopropylacrylamide-*co*-*N*-acryloyl glycine), poly(NIPA-*co*-Ac-Gly); (2) poly(*N*-isopropylacrylamide-*co*-*N*-acryloyl- $\beta$ -alanine), poly(NIPA-*co*-Ac- $\beta$ -Ala); (3) poly(*N*-isopropylacrylamide-*co*-*N*-acryloyl-4-amino butyric acid), poly(NIPA-*co*-Ac-4ABA); (4) poly(*N*-isopropylacrylamide-*co*-*N*-acryloyl-6-amino caproic acid), poly(NIPA-*co*-Ac-6ACA); and (5) poly(*N*-isopropylacrylamide-*co*-*N*-acryloyl-11-amino undecanoic acid), poly(NIPA-*co*-Ac-11AUA).

### 3.4. Conjugation of *p*-aminobenzamide to carboxyl groups of copolymers

PABA was covalently linked to the pendant carboxyl groups of these polymers via the amide link using water soluble carbodiimide [10,11]. PABA.2HCl was treated with 40-fold molar excess of sodium acetate in water to free the *p*-amino groups. Four grams of polymer were dissolved in 40 ml of double distilled water at 4–10°C, and CMC and PABA were added to it. The reaction mixture was stirred at 4–10°C for 12 h. The molar ratios of CMC:carboxyl groups and PABA:carboxyl groups were both 10:1. The PABA-linked polymer was precipitated by increasing the temperature above its LCST. The polymer was washed three times with cold double distilled water and dried under vacuum at room temperature.

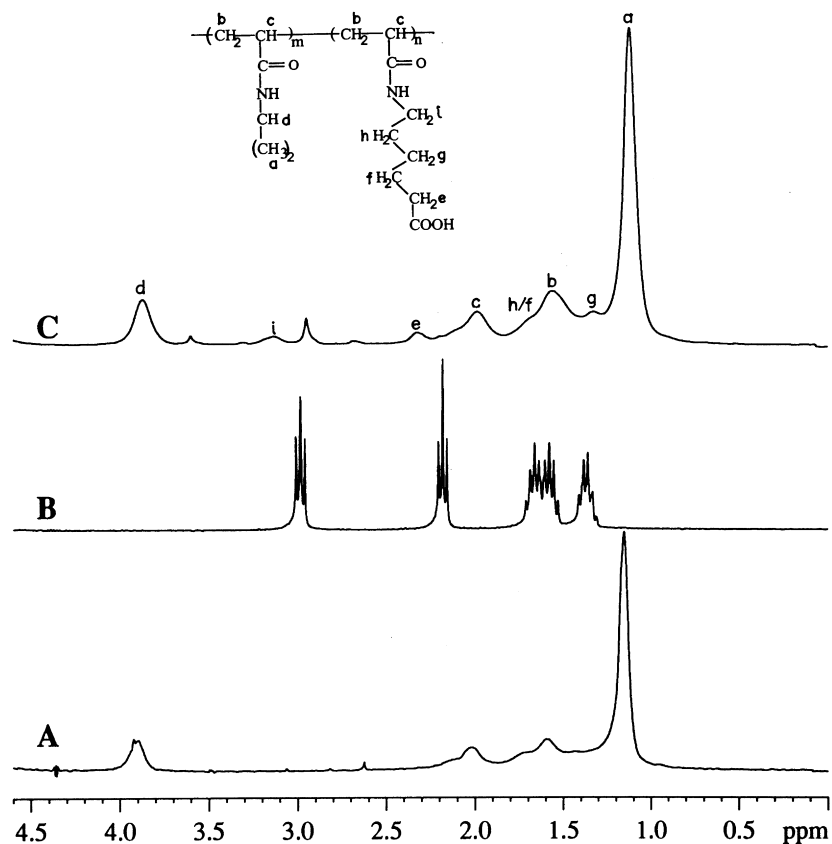


Fig. 1.  $^1\text{H}$  NMR spectrum of poly(NIPA) (A), 6-amino caproic acid (B) and poly(NIPA-co-Ac-6ACA) (C) in  $\text{D}_2\text{O}$ . A  $45^\circ$  flip angle of  $8\ \mu\text{s}$  with 15 s acquisition delay was used to accumulate 16 scans. The assignments of the peaks are indicated in (C).

### 3.5. NMR investigations

The concentration of all polymer samples used was  $30\ \text{mg ml}^{-1}$  in  $\text{D}_2\text{O}$ . The  $^1\text{H}$  NMR spectral and relaxation ( $T_1$ ) measurements were carried out on a Bruker MSL-300 FT-NMR spectrometer operating at the Larmor frequency of 300.13 MHz for protons.  $45^\circ$  pulse of  $8\ \mu\text{s}$  and an acquisition delay of 15 s were used for  $^1\text{H}$  spectral accumulations. A “ $\pi$ - $\tau$ - $\pi/2$ —acquisition” inversion recovery sequence was used for  $T_1$  measurements and the FT data were fitted using the online Bruker software SIMFIT. The temperature of the sample was precisely controlled using a Bruker BVT-1000 variable temperature controller and air/cold  $\text{N}_2$  gas flow system. The  $^1\text{H}$ - $^1\text{H}$  2D NOESY experiments were carried out at  $19^\circ\text{C}$  in the phase-sensitive mode using the time proportionate phase increment (TPPI) procedure [12–14]. In these experiments, no solvent suppression scheme was used. The  $\pi/2$  pulse was  $15\ \mu\text{s}$ . The 2D data processing was carried out using the xWINNMR software on a remote INDY workstation. The 2D  $^1\text{H}$ - $^1\text{H}$  NOESY experiments were also carried out on a Bruker DRX 500 FT-NMR spectrometer operating at the Larmor frequency of 500.13 MHz for protons. The NOESY pulse sequence incorporates a WATERGATE solvent suppression scheme [15,16] and the 2D data were acquired in the phase sensitive mode using TPPI scheme. A  $90^\circ$  pulse of  $11.5\ \mu\text{s}$  and gradient

pulse of 1 ms were used for these experiments. The relevant acquisition and processing details are given in the figure captions. The proton chemical shifts are referenced to external TMS (tetramethylsilane) as the standard at 0 ppm.

## 4. Results and discussion

### 4.1. $^1\text{H}$ NMR spectra and temperature dependence

The  $^1\text{H}$  NMR spectra of poly(NIPA) (A), the 6ACA monomer (B) and the poly(NIPA-Ac-co-6ACA) polymer (C) in  $\text{D}_2\text{O}$  are shown in Fig. 1. The assignments of the proton resonances for pure poly(NIPA) are based on earlier work and especially the  $^1\text{H}$ - $^{13}\text{C}$  HETCOR study by Zeng et al [17]. The peak assignments in Fig. 1(B) are straightforward. The  $^1\text{H}$  spectrum of the copolymer (C) is an addition of spectra in (A) and (B) except for a slight change in chemical shift for the 6ACA signals. On the other hand, we find that in all the poly(NIPA)-copolymer systems studied, the proton resonances of poly(NIPA) occur at the same chemical shift. The resonances are sharp and well resolved.  $^1\text{H}$  resonances for the 6ACA monomer in (B) are broadened in (C) ( $\delta\nu \sim 20\ \text{Hz}$ ), confirming that the monomer is incorporated in the polymer. Based on the spectral deconvolution of peaks in (C) and comparison with the

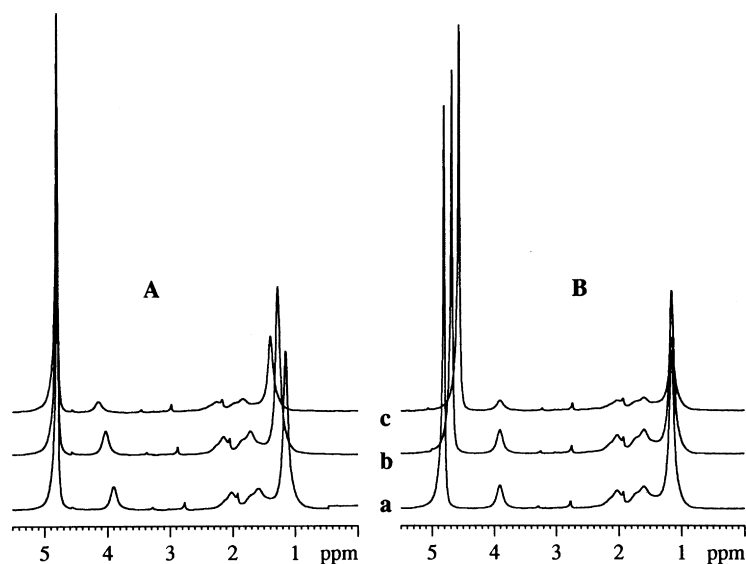


Fig. 2. Temperature dependence of the  $^1\text{H}$  NMR spectra of poly(NIPA-co-Ac-PABA, 70:30) in  $\text{D}_2\text{O}$  at 19°C (a), 29°C (b) and 39°C (c) using  $^2\text{H}$  lock (A) and without  $^2\text{H}$  lock (B).

amount of Ac-6ACA in the feed, we conclude that 95% of the monomer is incorporated in the polymer.

Having assigned the peak positions we wished to investigate the temperature dependence of the spectrum in the region below LCST before we could traverse LCST. Since we wanted to cover a wider temperature range, we selected the polymer poly(NIPA-co-Ac-PABA, 70:30) which has an LCST of 54°C. The proton NMR resonances of this polymer in the range 19–39°C are shown in Fig. 2(A). These results indicate a shift in the peak at 1.15 ppm to lower field values with increasing temperature. These results are consistent with the findings reported by Zeng et al. [17] for poly(NIPA) in solution in the temperature range 28–35°C and by Tokuhiro et al [18] for non-ionic poly(*N*-isopropylacrylamide) gels in the temperature range 2.4–32.7°C. The phase separation at the LCST involves coil to globule transition of the single chain slightly below LCST followed by the inter-chain aggregation [6]. Since the highest temperature at which we recorded the spectrum (39°C) is well below the LCST of the polymer (54°C), we did not anticipate significant conformational changes in the polymer in the temperature range investigated. This was also confirmed by nOe experiments, which showed that incorporation of Ac-6ACA or Ac-PABA did not influence the cross peaks between the main chain and side chain protons (see later).

To examine if this was an artifact arising from the  $^2\text{H}$  lock used, we reinvestigated the spectra at three temperatures without using a  $^2\text{H}$  lock. In the unlocked mode, the water resonance clearly shifts to a higher field due to the temperature dependence of the chemical shift of water (Fig. 2(B)). The temperature dependence of the water resonances has also been reported by Gottlieb et al [19]. We therefore conclude that, in the  $^2\text{H}$  lock experiment the frequency shift of water resonance caused by the increase in tempera-

ture is instantaneously restored by the  $^2\text{H}$  lock to the set field frequency lock condition, thus making it appear as if the polymer resonances have shifted as reported by earlier researchers.

#### 4.2. LCST of poly(NIPA) copolymers

Numerous methods such as light scattering, differential scanning calorimetry, turbidometry and fluorescence spectroscopy have been used to estimate the LCST of thermo-reversible polymers [4]. NMR techniques have also been used to investigate the LCST phenomenon in poly(NIPA) and its copolymers [17,18,20–27]. The use of NMR has an advantage, in that, unlike other methods such as light scattering and turbidometry, it can be used to follow the LCST behaviour of graft and block copolymers in which each component exhibits LCST behaviour. Additionally, NMR gives an accurate profile of the LCST since it detects the phenomenon at the molecular level.

In order to monitor the LCST of poly(NIPA) copolymers, we recorded the  $^1\text{H}$  NMR spectra of poly(NIPA) and eleven different copolymer systems. Fig. 3 is a representative proton spectrum of poly(NIPA-co-Ac-6ACA, 90:10) at various temperatures. It is found that as the temperature is raised, the intensity of the  $^1\text{H}$  resonances shows a sudden decrease in the temperature range 26–30°C. The temperature response of  $^1\text{H}$  NMR spectra in cross-linked poly(NIPA) hydrogels has been studied earlier through linewidth measurement [26]. For the thermo-sensitive polymer in the gel state, increase in the temperature leads to deswelling and the degree of collapse is measured by the decrease in the swelling ratio. This results in a decrease in the molecular mobility of the polymer segments and broadening of the proton lines. Subsequently, Yoshioka et al. [27]

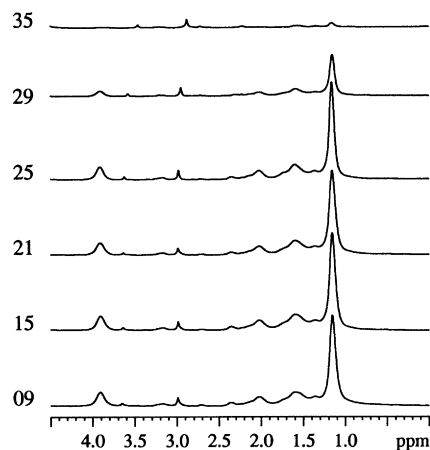


Fig. 3. Monitoring of LCST behaviour of the poly(NIPA-*co*-Ac-6ACA, 90:10) by  $^1\text{H}$  NMR. The temperature ( $^{\circ}\text{C}$ ) of the measurement is indicated in the respective spectrum.

too reported similar linewidth broadening during LCST transition of the hydrogels comprising poly(NIPA-*co*-PEG). For a linear polymer the increase in temperature leads to a coil to globule transition as well as the inter-polymer aggregation resulting in phase separation [6]. In the solution mode  $^1\text{H}$  NMR measurement, the solid phase remains undetected. We therefore believe that the area under the signal can be conveniently used to monitor the transition process. A plot of the signal area as a function of temperature, for the copolymer poly(NIPA-*co*-Ac-6ACA, 90:10), shown in Fig. 4, clearly depicts the LCST transition at  $28^{\circ}\text{C}$ , which is in good agreement with the value of  $27^{\circ}\text{C}$  obtained by turbidometric measurement. The results for other systems are summarized in Table 1.

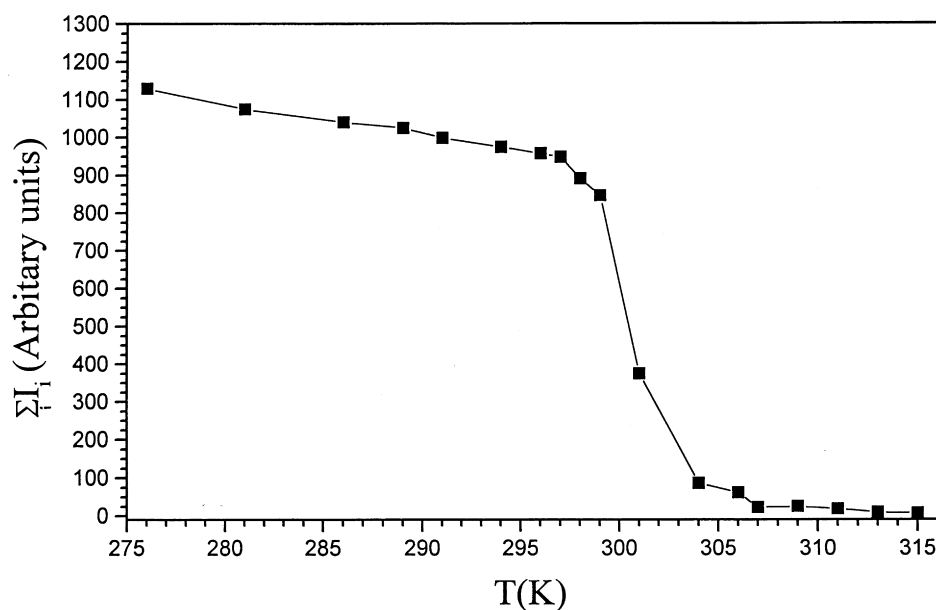


Fig. 4. Temperature dependence of the total polymer signal area of poly(*N*-isopropylacrylamide-*co*-6ACA, 90:10).

Table 1  
Comparison of LCSTs recorded by the  $^1\text{H}$  NMR and turbidometric methods

| Polymers                                            | LCST ( $^{\circ}\text{C}$ ) by |              |
|-----------------------------------------------------|--------------------------------|--------------|
|                                                     | NMR                            | Turbidometry |
| Poly(NIPA)                                          | 32                             | 32           |
| Poly(NIPA- <i>co</i> -Ac-PABA, 70:30)               | 54                             | 53           |
| Poly(NIPA- <i>co</i> -Ac-6ACA, 90:10)               | 28                             | 27           |
| Poly(NIPA- <i>co</i> -Ac-6ACA, 80:20)               | 22                             | 23           |
| Poly(NIPA- <i>co</i> -Ac-6ACA-PABA, 90:10)          | 41                             | 41           |
| Poly(NIPA- <i>co</i> -Ac-4ABA, 90:10)               | 36                             | 36           |
| Poly(NIPA- <i>co</i> -Ac-4ABA-PABA, 90:10)          | 53                             | 55           |
| Poly(NIPA- <i>co</i> -Ac-Gly, 90:10)                | 35                             | 34           |
| Poly(NIPA- <i>co</i> -Ac-Gly-PABA, 90:10)           | 38                             | 36           |
| Poly(NIPA- <i>co</i> -Ac- $\beta$ -Ala, 90:10)      | 34                             | 33           |
| Poly(NIPA- <i>co</i> -Ac- $\beta$ -Ala-PABA, 90:10) | 36                             | 35           |
| Poly(NIPA- <i>co</i> -Ac-11AUA, 90:10)              | 34                             | 34           |
| Poly(NIPA- <i>co</i> -Ac-11AUA-PABA, 90:10)         | 36                             | 35           |

As seen in Fig. 4, the LCST transition zone is encompassed by two plateau regions in which the area practically remains constant. Clearly, the signal area does not reach zero at temperatures above the LCST, suggesting thereby that a small fraction of low molecular weight species still remains in solution. The origin of these signals due to the presence of the soluble polymer was further independently confirmed by collapsing the copolymer above the LCST, decanting the solution and analysing the solution by proton NMR which confirmed the presence of the same resonances. The thermo-reversible nature of the LCST transition is also reflected through  $^1\text{H}$  area measurements. An inspection of the LCST of various poly(NIPA)-copolymer systems (see Table 1) shows that copolymerization of NIPA with acryloyl amino acids of increasing chain lengths and conjugation with *p*-aminobenzamidine leads to *N*-isopropylacrylamide

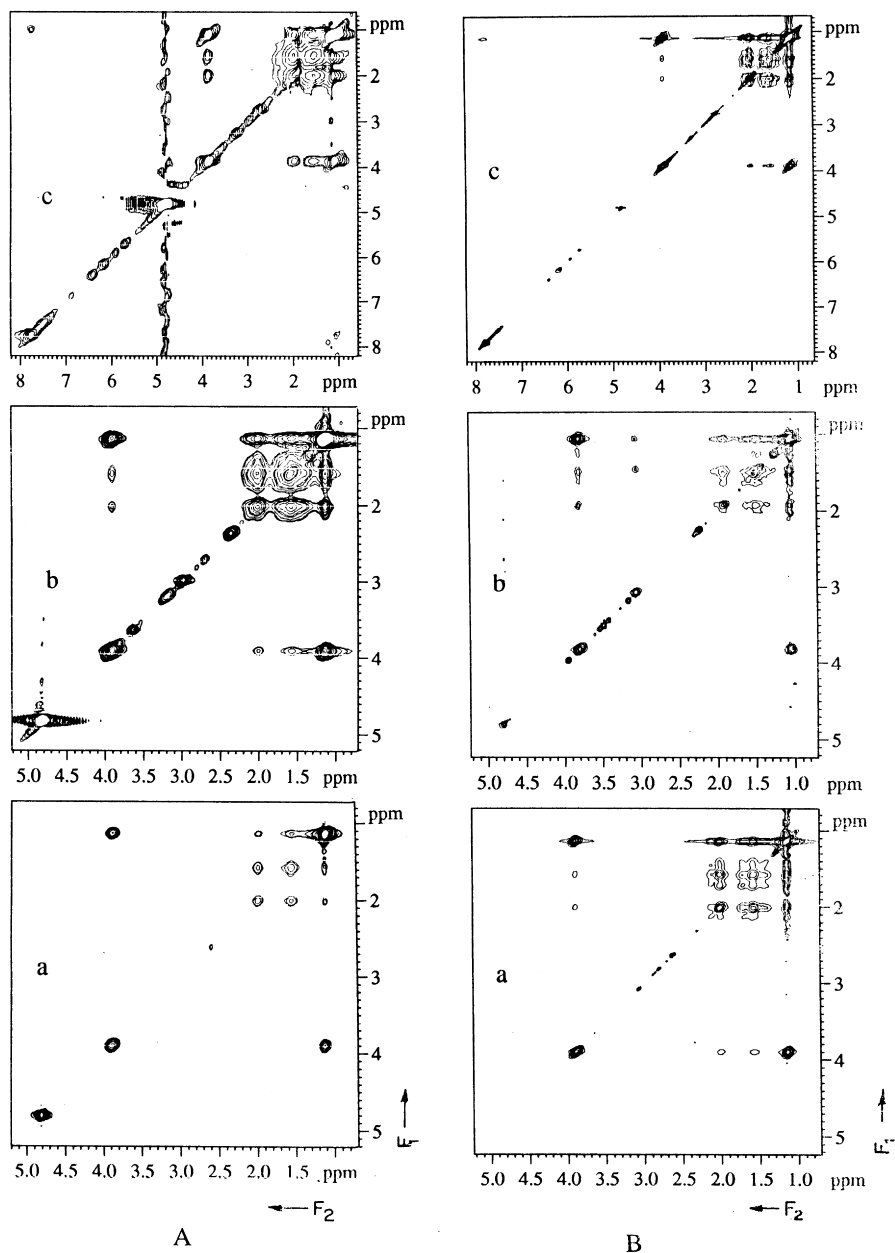


Fig. 5.  $^1\text{H}$ - $^1\text{H}$  2D NOESY plots of poly(NIPA) (a), poly(NIPA-co-Ac-6ACA, 80:20) (b) and poly(NIPA-co-Ac-PABA, 70:30) (c) without water suppression at 300 MHz (A) and with water suppression at 500 MHz (B). A mixing time of 500 ms was used. Proton  $90^\circ$  pulse of  $15\ \mu\text{s}$  and  $11.5\ \mu\text{s}$  were used for the experiments without and with water suppression, respectively. 256 experiments for (A) and 1024 experiments for (B) were performed along the  $t_1$  dimension. The data was processed with exponential multiplication along  $F_2$  and sine square bell along  $F_1$ .

polymers exhibiting a wide range of LCSTs. Increasing the hydrophobicity of the polymers, e.g. poly(NIPA-co-Ac-6ACA, 80:20) leads to the lowering of the LCST ( $22^\circ\text{C}$ ) and increasing the hydrophilicity, e.g. poly(NIPA-co-Ac-PABA, 70:30) leads to the enhancement in LCST ( $54^\circ\text{C}$ ) as anticipated.

It is also observed that at a given copolymer composition (90:10), the LCST of the copolymer of NIPA and acryloyl amino acid cannot be directly correlated with the methylene chain length in the amino acid. This is because apart from the methylene group content, the location of the group

within the monomer structure influences the LCST behaviour of the polymer [7].

#### 4.3. $^1\text{H}$ - $^1\text{H}$ 2D NOESY experiments and analysis

In order to understand the nature of molecular association that may be responsible for the LCST changes observed in the poly(NIPA)-copolymer systems, we investigated the copolymers of poly(NIPA), namely poly(NIPA-co-Ac-6ACA, 80:20) and poly(NIPA-co-AC-PABA, 70:30) by  $^1\text{H}$ - $^1\text{H}$  2D NOESY experiments. We chose to study these

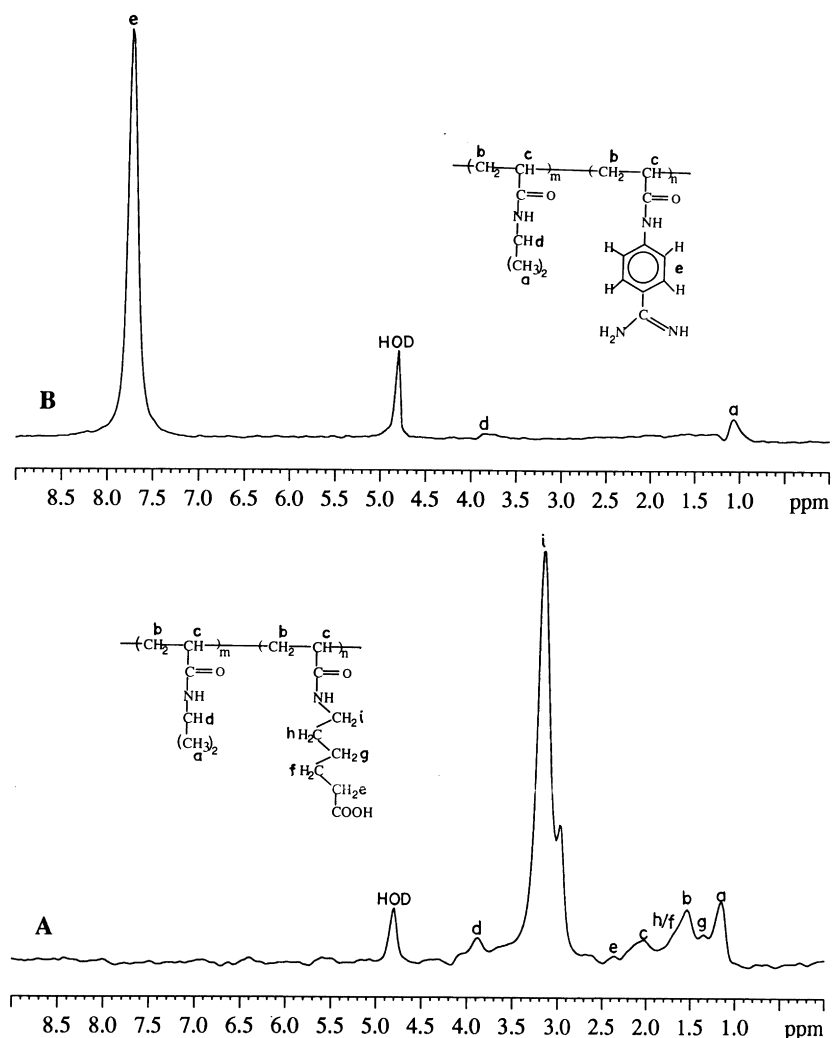


Fig. 6. Cross-sections of the rows from the 2D NOESY spectrum of poly(NIPA-co-Ac-6ACA, 80:20). (A) At 3.02 ppm which reflects inter-chain dipolar interactions of 6ACA within itself and with NIPA moiety. (B) A cross-section of the row in poly(NIPA-co-Ac-PABA, 70:30) at 7.75 ppm proton arising from PABA.

systems at a constant reference temperature (19°C), well below the LCST of both polymers. The 2D NOESY experiment provides a convenient way of monitoring the interactions between the various protons in the copolymer system. Since the NOESY cross-peak development is due to the through-space dipole–dipole interaction and has an inverse sixth power dependence on distance, long and short range interactions, can be clearly delineated in the 2D NOESY experiment. In Fig. 5, we show the phase-sensitive 2D NOESY contour plots of poly(NIPA) (a), poly(NIPA-co-Ac-6-ACA, 80:20) (b) and poly(NIPA-co-Ac-PABA, 70:30) (c) at 7.01 and 11.5 T (A and B, respectively). The optimum mixing time ( $\tau_m$ ) was found to be 500 ms by studying the mixing time dependence of the cross-peak development in poly(NIPA).

For poly(NIPA), the 2D contour plots establish dipolar correlation between the protons within the main chain, between the protons of the isopropyl group and between the protons in the main chain and the isopropyl group.

Since the cross-peaks are of the same phase as the diagonal peaks (positive cross-peaks), the nOe is negative and occurs essentially in the long correlation limit ( $\omega_0\tau_c \gg 1$ ) [28]. The larger development of nOe in this so-called ‘spin diffusion’ regime, is clearly reflected by the strong intra-molecular cross-peak development noticed in the figure. Due to the strong ridge of water resonance especially along  $F_1$ , the polymer–water interaction could not be detected unambiguously in the 2D spectra. Moreover, the polymer backbone protons and the protons of the isopropyl group are known to be hydrophobic and hence the polymer–water interactions are expected to be greatly attenuated.

For poly(NIPA-co-Ac-6ACA, 80:20) which exhibits a LCST of 22°C, the dipolar correlations within the poly(NIPA) part remain largely unaltered, suggesting that the cross-relaxation behaviour is little influenced by the introduction of Ac-6ACA (Fig. 5(b) in both A and B). Similarly, intra-molecular cross-peaks within the 6ACA protons are strongly developed and occur with a positive sign. The

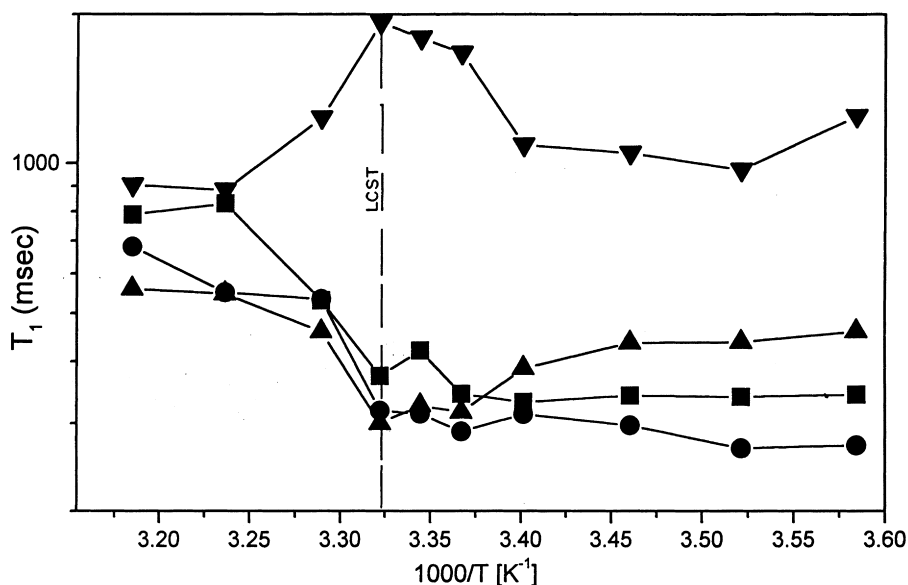


Fig. 7. A semilog plot of the temperature dependence of proton  $T_1$  for poly(NIPA-co-Ac-6ACA, 90:10). (■) methyl protons of poly(NIPA), (▲) backbone methylene protons in poly(NIPA), (●) protons attached to the  $\gamma$ -carbon in Ac-6ACA (g) in Fig. 1) and (▼) the methine proton of the isopropyl group in the poly(NIPA).

strong cross-peaks between the  $\alpha$ -protons of 6ACA side chain ('i' in Fig. 1(C)) and poly(NIPA) signals of the backbone as well as side chain protons are also noticed. For poly(NIPA-co-Ac-PABA, 70:30) the cross-peaks between PABA protons and protons belonging to the poly(NIPA) are seen (Fig. 5(c) in both). A similar feature for the poly(NIPA) cross peaks development was found in this system. Additionally, it shows cross peaks between ring protons of the PABA and poly(NIPA) side chain.

The intra-molecular dipolar interaction between the copolymer unit and the poly(NIPA) chain is easily visualized by an inspection of the 1D spectra extracted as rows from the 2D data set of Fig. 5(a) at the representative chemical shift positions for the 3.02 ppm proton signal of 6-ACA and 7.75 ppm proton signal of PABA. This is shown in Fig. 6(A) and (B), respectively, with the peak assignments. This helps us to select proton environments in the two copolymer systems that show dipolar correlations with the protons of poly(NIPA). The resonances arising from the NIPA units in poly(NIPA-co-Ac-6ACA, 80:20) are stronger (Fig. 5(a)) than those in poly(NIPA-co-Ac-PABA, 70:30), indicating

stronger intra-chain dipolar interactions between Ac-6ACA and NIPA than those between PABA and NIPA. As mentioned before, due to the dominance of the water ridge in the 2D spectrum (4.8 ppm) we were unable to monitor the polymer–water interaction. Hence an unequivocal verification for a stronger polymer–solvent interaction in PABA over 6ACA, could not be obtained. The increased overall polymer–polymer interaction explains the lowering of the LCST due to incorporation of Ac-6ACA vis a vis Ac-PABA with reference to poly(NIPA). The variations in the LCSTs of polymers and copolymers due to hydrogen bonding interactions have been investigated by IR spectroscopy [7]. The NMR investigations demonstrate the contribution due to hydrophobic interactions to the LCST of copolymers.

#### 4.4. Proton spin–lattice relaxation ( $T_1$ ): measurements and interpretation

Fig. 7 represents the temperature dependence of proton spin–lattice relaxation time ( $T_1$ ) for the four distinct proton resonances, which belong to the repeat unit

Table 2  
Proton spin-lattice relaxation data of homo and copolymers of NIPA

| Peaks                      | $T_1$ (s)  |                              |                              |                              |
|----------------------------|------------|------------------------------|------------------------------|------------------------------|
|                            | Poly(NIPA) | Poly(NIPA-Ac-co-6ACA, 90:10) | Poly(NIPA-Ac-co-6ACA, 80:20) | Poly(NIPA-Ac-co-PABA, 70:30) |
| CH (isopr.)                | 1.37       | 1.16                         | 0.877                        | 1.173                        |
| CH (backbone)              | 0.691      | 0.656                        | 0.579                        | 0.655                        |
| CH <sub>2</sub> (backbone) | 0.564      | 0.510                        | 0.419                        | 0.529                        |
| CH <sub>3</sub>            | 0.611      | 0.595                        | 0.528                        | 0.596                        |



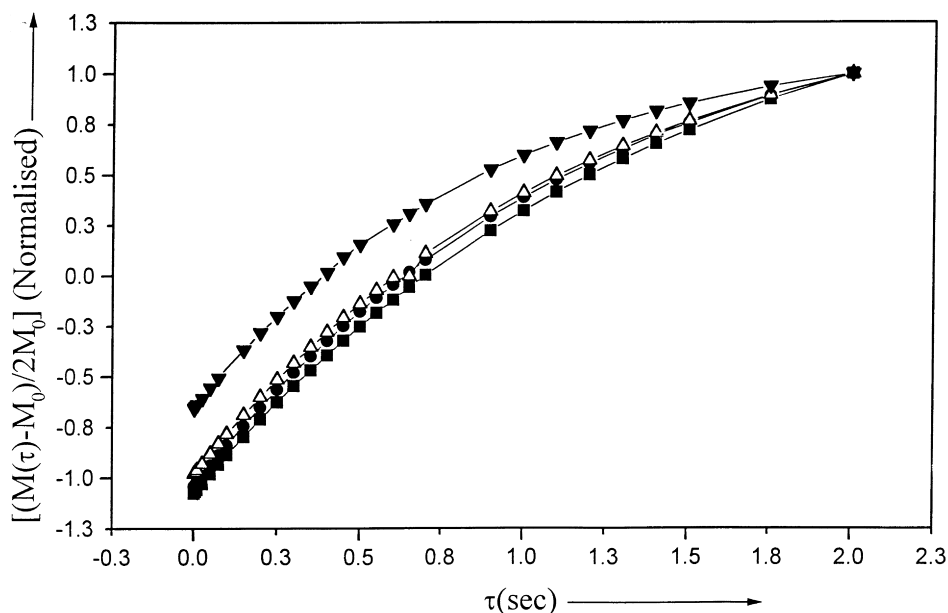


Fig. 8. Inversion-recovery of the lone proton of isopropyl CH in poly(NIPA) (■), poly(NIPA-*co*-Ac-6ACA, 90:10) (△), poly(NIPA-*co*-Ac-6ACA, 80:20) (▼), poly(NIPA-*co*-Ac-PABA, 70:30) (●). An incremental delay of 500  $\mu$ s to 2 s was used to accumulate 8 scans. Processing was done using Bruker SIMFIT program.

of poly(NIPA-*co*-Ac-6ACA, 90:10). Clearly, the  $T_1$  behaviour is found to be different for different resonances. Typically, a larger change in  $T_1$  is noticed near the LCST, especially for the CH proton of the isopropyl group which increases with temperature. This trend is in agreement with the observations made by Tokuhiko et al. [18] and Zeng et al. [17]. The  $T_1$  behaviour of other protons shows an increase (isopropyl CH<sub>3</sub> and  $\gamma$ -CH<sub>2</sub> of 6 ACA) or a decrease (backbone CH<sub>2</sub>) over the temperature range below the LCST. Beyond the LCST, the  $T_1$  measurements merely reflect the behaviour of the low molecular weight species that remain in the solution, because for the phase separated solid copolymer no  $T_1$  measurements can be made in our experiment. It is interesting to note the lone isopropyl proton  $T_1$  value for the poly(NIPA) solution is 1.37 s at 22°C, compared to the  $T_1$  value of 766 ms reported by Badiger et al. [26] in the gel state. This is presumably due to the restricted molecular mobility in the gel state.

We measured the  $T_1$  values at 21°C for poly(NIPA) and its copolymers containing increasing 6ACA content. The results are summarized in Table 2. The inversion-recovery experimental data are shown in Fig. 8.  $T_1$  values decrease with increasing Ac-6ACA content. The methylene groups in 6ACA enhance hydrophobic interactions with the isopropyl group in NIPA, thus lowering the  $T_1$  and also lower the LCST of the copolymer. This interaction possibly dominates over the hydrophilic interaction between the terminal carboxyl group and water, which was not monitored.

In contrast, in the case of poly(NIPA-*co*-Ac-PABA, 70:30), the interaction between the ring protons in PABA and the isopropyl groups in NIPA results in the lowering of  $T_1$  as in the case of poly(NIPA-*co*-Ac-6ACA). The evidence

for such an interaction in poly(NIPA-*co*-Ac-PABA) can be seen in the 2D <sup>1</sup>H-<sup>1</sup>H NOESY spectrum (Figs. 5(C) and 6(B)) as weak cross peaks between the isopropyl protons of the NIPA and the ring protons of PABA. However, this has not resulted in a corresponding decrease in the LCST. This can be the result of the highly hydrophilic guanidino group, the interactions of which were not monitored since the protons of the guanidino group exchange with deuterium. The role of the interactions between the guanidino group in PABA and water in enhancing the LCST can be elucidated by incorporating substituted benzamidines such as 4-vinyl-benzamide. In these cases, the possible interactions of methylene groups of the guanidino groups will lead to additional interactions with the isopropyl groups and hence suppress the polymer-solvent interactions. In these systems one would expect a decrease in the LCST and a decrease in  $T_1$  as observed in the copolymers of NIPA and Ac-6ACA here.

## 5. Conclusions

We have synthesized copolymers of NIPA and acryloyl amino acids which exhibit LCST in the range 22–54°C. The distinct <sup>1</sup>H resonances of poly(NIPA) and the copolymer have been resolved and the LCST behaviour has been monitored through <sup>1</sup>H NMR. <sup>1</sup>H-<sup>1</sup>H 2D NOESY spectroscopy provides insights into the relative importance of polymer-polymer and polymer-solvent interactions that govern the observed LCST behaviour. This is also confirmed by independent  $T_1$  measurements on poly(NIPA-*co*-Ac-6ACA, 90:10) exhibiting LCST at 28°C. The predominance of the

polymer–polymer interactions in poly(NIPA-*co*-Ac-6ACA, 90:10), than that in poly(NIPA-*co*-Ac-PABA, 70:30) is attributed to the increased hydrophobicity in the former and increased hydrophilicity in the latter. The molecular associations responsible for the observed LCST behaviour, which can provide valuable guidelines for tailoring polymers for applications in affinity based separations, drug delivery systems etc. have been highlighted.

## References

- [1] Taylor LD, Cerankowski LD. *J Polym Sci, Polym Chem Ed* 1975;13:2551–70.
- [2] Heskins M, Guillet JE. *J Macromol Sci, Chem* 1968;A2:1441–55.
- [3] Galaev IY, Mattiasson B. *Enzyme Microb Technol* 1993;15:354–66.
- [4] Schild HG. *Prog Polym Sci* 1992;17:163–249.
- [5] Vaidya AA, Lele BS, Kulkarni MG, Mashelkar RA. *Biotech Bioeng* 1999;34(4):418–25.
- [6] Qiu X, Li M, Kwan CMS, Wu C. *J Polym Sci Part B (Polym Phys)* 1998;36:1501–6.
- [7] Plate NA, Lebedeva TL, Valuev LI. *Polym J* 1999;31(1):21–7.
- [8] Male KB, Luong JHT, Nguyen AL. *Enzyme Microb Technol* 1987;9:374–8.
- [9] Pecs M, Eggert M, Schugerl K. *J Biotechnol* 1991;21:137–42.
- [10] Papisov MI, Maksimenko AV, Torchilin VP. *Enzyme Microb Technol* 1985;7:11–6.
- [11] Szajani B, Sudi P, Klamar G, Jaszay ZM, Petnehazy I, Toke L. *Appl Biochem Biotechnol* 1991;30:225–31.
- [12] Redfield AG, Kunz SD. *J Magn Reson* 1986;66:410–7.
- [13] Bodenhausen G, Vold RL, Vold RR. *J Magn Reson* 1980;37:93–106.
- [14] Marion D, Wüthrich K. *Biochem Biophys Res Commun* 1983;113:967–75.
- [15] Piotto M, Saudek V, Sklenar V. *J Biomol NMR* 1992;2:661–6.
- [16] Sklenar V, Piotto M, Leppik R, Saudek V. *J Magn Reson A* 1993;102:241–5.
- [17] Zeng F, Chen T, Feng H. *Polymer* 1997;38(22):5539–44.
- [18] Tokuhito T, Takayuki A, Mamadu A, Tanaka T. *Macromolecules* 1991;24:2936–43.
- [19] Gottlieb HE, Kotlyar V, Neudelman A. *J Org Chem* 1997;62:7512–5.
- [20] Ohta H, Ando I, Fujishige S, Kubota K. *J Polym Sci Part B (Polym Phys)* 1991;29:963–8.
- [21] Ganapathy S, Rajamohanam PR, Ray SS, Mandhare AB, Mashelkar RA. *Macromolecules* 1994;37(12):3432–5.
- [22] Case BL, Liu Ys, Bergbreiter DE. *Polym Prepr* 1998;39(1):298–9.
- [23] Franzin CM, Macdonald PM, Polozova A, Winnik FM. *Biochem Biophys Acta* 1998;1415(1):219–34.
- [24] Ray SS, Rajamohanam PR, Badiger MV, Devotta I, Ganapathy S, Mashelkar RA. *Chem Engng Sci* 1998;53(5):869–77.
- [25] Tanaka N, Matsukawa S, Kurosu H, Ando I. *Polymer* 1998;39(20):4703–6.
- [26] Badiger MV, Rajmohanam PR, Kulkarni MG, Ganapathy S, Mashelkar RA. *Macromolecules* 1991;24:106–11.
- [27] Yoshioka H, Mori Y, Cushman JA. *Polym Adv Technol* 1994;5(2):122–7.
- [28] Neuhaus D, Williamson M. The nuclear overhauser effect in structural and conformational analysis, VCH, 1989. p. 263.